Bioorganic & Medicinal Chemistry 18 (2010) 6538–6546

Contents lists available at ScienceDirect

Bioorganic & Medicinal Chemistry

journal homepage: www.elsevier.com/locate/bmc

Synthesis and ribonuclease A inhibition activity of resorcinol and phloroglucinol derivatives of catechin and epicatechin: Importance of hydroxyl groups

Sansa Dutta, Amit Basak *, Swagata Dasgupta *

Department of Chemistry, Indian Institute of Technology, Kharagpur 721 302, India

ARTICLE INFO

Article history:
Received 17 May 2010
Revised 18 June 2010
Accepted 19 June 2010
Available online 25 June 2010

Keywords:
Catechin
Epicatechin
Inhibition
RNase A
Angiogenin
CAM assay

ABSTRACT

The reported ribonuclease A inhibitory activity of the green tea extracts prompted us to synthesize novel catechin/epicatechin based conjugates with resorcinol and phloroglucinol with the aim to increase the number of phenolic OH groups. These are found to be more effective inhibitors of ribonuclease A as compared to catechin and epicatechin thus indicating the importance of number of phenolic OH groups for the inhibition of ribonucleolytic activity. Fluorescence studies have been carried out to evaluate the binding parameters. The protein–ligand docking studies are also performed to gain insight into the protein–polyphenols interactions. The epicatechin based polyphenols **1** and **2** also showed inhibition of angiogenin-induced angiogenesis, as determined by chorioallantoic membrane (CAM) assay.

1. Introduction

Replication, transcription and translation form the basis of all life processes. The genetic flow of information is controlled by DNA polymerases involved in DNA replication, RNA polymerases for RNA synthesis and RNA depolymerases (usually called 'ribonucleases') for RNA degradations. Mammalian Ribonucleases (RNases) are endonucleases that catalyze the degradation of RNA via a two-step transphosphorylation-hydrolytic reaction.[1,2] RNases can be cytotoxic because undesired cleavage of RNA renders its encoded information undecipherable. They inhibit the translation processes that subsequently cause cell death by adsorbing specifically to certain cells, entering the cytosol and degrading the RNA. Hence, the past few years has seen a surge in the search for low molecular weight inhibitors of ribonucleases. This has also been stimulated largely by research demonstrating that several pancreatic RNase A homologues, including angiogenin,[3] eosinophil-derived neurotoxin (EDN),[4] and bovine seminal RNase A,[5] utilize their enzymatic activities for potent physiological effects.[6] The ribonucleolytic centre of RNase A consists of multiple subsites (e.g., P_1, B_1 and B_2) that bind to the phosphate, nucleobase and ribose components of RNA molecule, respectively. However, the cleavage of phosphodiester bond occurs at the P_1 site comprising of His 12, Lys 41 and His 119. Apart from the amino acid residues directly involved in the catalytic process, residues present at various subsites are known to play an indirect role in the catalytic mechanism. So a strategy can be adopted such that the inhibitors target these subsites other than the active site resulting in the loss of enzymatic activity. Ribonuclease inhibitors, either synthetic or natural, have been intensively sought after for therapeutic purposes. This also finds application in angiogenesis research. The primary reason is that angiogenesis is frequently promoted by angiogenin, a pancreatic ribonuclease homologue, and inhibition of angiogenin is expected to result in suppression of growth and metastasis of solid tumours. The ribonucleolytic activity of angiogenin is essential for its angiogenic activity. It is speculated that these inhibitors may also be used in a broader aspect to inhibit enzymes, like angiogenin, that belong to the ribonuclease superfamily.

In this regard, polyphenols, once known as Vitamin P, have drawn keen interest because of possible health benefits of all types of polyphenols. Recent studies indicate that polyphenols may have antioxidant characteristics with potential health benefits[7] and that they may reduce the risk of cardiovascular disease and cancer.[8,9] The reports suggest that the green tea extracts comprising of epicatechin (EC), epigallocatechin (EGC), epicatechin gallate (ECG) and epigallocatechin gallate (EGCG) showed inhibition of ribonucleolytic activity of ribonuclease A and the order of inhibition is EGCG > ECG > EGC > EC.[10,11] The earlier studies have prompted us to investigate whether increasing the number of phenolic hydroxyl groups in the form of phloroglucinol and resorcinol at C-4 in the

* Corresponding authors. Tel.: +91 3222 283300; fax: +91 3222 282252.
E-mail address: absk@chem.iitkgp.ernet.in (A. Basak).

0968-0896/$ - see front matter © 2010 Elsevier Ltd. All rights reserved.
doi:10.1016/j.bmc.2010.06.077

epicatechin/catechin skeleton has any effect on the inhibition of ribonuclease A. Based on this rationale, we embarked upon the synthesis of polyphenols (**1–4**) (Fig. 1). The C-4 position of catechin or epicatechin is important as most of the biologically active oligomers are linked via this position.

2. Results and discussion

2.1. Synthesis

The key step in the synthesis of the polyphenols **1–4** involved the formation of C–C bond involving the 4-position of catechin/epicatechin and the nucleophile. This was achieved by the reported[12] LiBr-mediated coupling of 4-acetoxy tetrabenzyl catechin or epicatechin and phloroglucinol/resorcinol. The polyphenols (**1**, **2**) were synthesized starting from (−)-epicatechin (EC) while (+)-catechin (C) served as the starting compound for **3** and **4**. The benzyl ether was chosen as the protecting group because its deprotection can be done under neutral conditions. Acid or base sensitive protecting groups were avoided because of possible racemization at C-2. The coupled products were purified by silica-gel column chromatography and the purified partially protected compounds were deprotected with H_2 in presence of Pearlman's catalyst[12] or 30% Pd–charcoal to afford the target compounds (Schemes 1A and 1B). These were purified by precipitation from methanol–ether.

The structure of various compounds was elucidated on the basis of NMR and mass spectrometric studies. The stereochemistry at C-4 was determined by comparing the J_{3-4} and J_{2-3} coupling constants in the partially protected compounds **9** and **10** with similar compounds **11–13** reported earlier by Roux and co-workers[13a] (Table 1) and others.[13b–d] The ^{1}H NMR spectra (taken in MeOH-d_4) in the final compounds **1–4** gave broad signals thus making it difficult to calculate the coupling constants and hence could not be used for comparison. The mass spectral data was also in conformity with the structure of the final compounds.

2.2. Enzyme inhibition

The inhibition of the ribonucleolytic activity of RNase A was initially checked by an agarose gel based assay where the degradation of tRNA by RNase A was monitored (Fig. 2A and B). The most intense band observed in the first lane is due to the presence of the control tRNA. The very faint band in the second lane (Fig. 2A) and third lane (Fig. 2B) indicates the complete degradation of tRNA by RNase A. The degree of inhibition of RNase A by the polyphenolic compounds (**1–4**), epicatechin, catechin and 3′-cytidine mono phosphate (3′-CMP), a known inhibitor of RNase A is ascertained from the differential intensity of residual tRNA in respective lanes in Figure 2A and B (relative intensity values with respect to the control are presented in tabular form). As the same inhibitor concentration was maintained for all the cases, compounds **1** and **3** are apparently more potent compared to compounds **2** and **4** as reflected in the relative intensity values obtained from the gel (Table 2). Moreover, the faint band of tRNA in Figure 2A and B corresponding to that of catechin (C) and epicatechin (EC) supports the fact that incorporating greater number of phenolic hydroxyl groups in the polyphenolic system increases efficacy of the synthesized compounds in the inhibition of ribonuclease A.

The inhibition of the ribonucleolytic activity of RNase A by the polyphenols was further confirmed quantitatively by a precipitation assay.[14] Here the amount of cleaved tRNA is assessed spectrophotometrically at 260 nm .The hydrolysed fragments of the tRNA formed

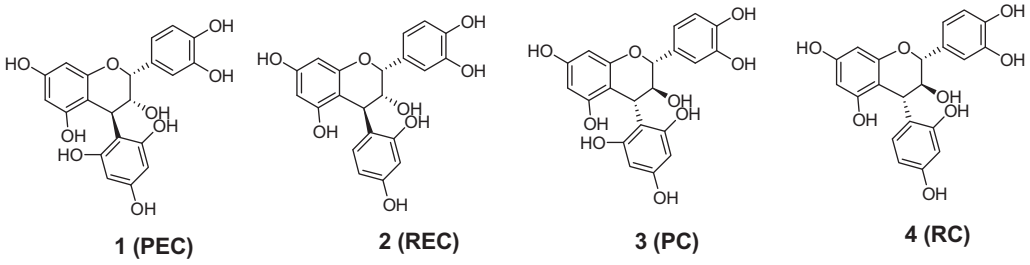

Figure 1. The target polyphenols **1–4**.

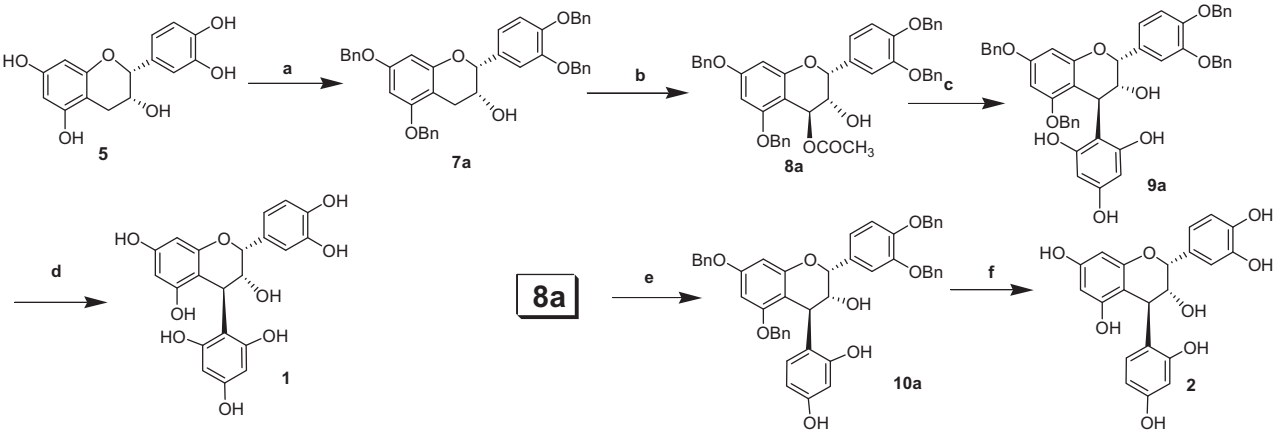

Scheme 1A. Synthesis of polyphenols (**1–2**) from epicatechin. Reagents and conditions: (a) BnBr, K_2CO_3, DMA, rt, 24 h; (b) $Pb(OAc)_4$, benzene/acetic acid (1:1), rt, 18 h; (c) phloroglucinol, LiBr, THF/DCM (1:1), reflux, 70 °C, 24 h; (d) 20% $Pd(OH)_2$–C, THF/MeOH/H_2O (20:1:1), H_2 (2 bar), 4 h; (e) resorcinol, LiBr, THF/DCM (1:1), reflux, 70 °C, 24 h; (f) 30% Pd–C, dry ethanol, H_2 (2 bar), 4 h.

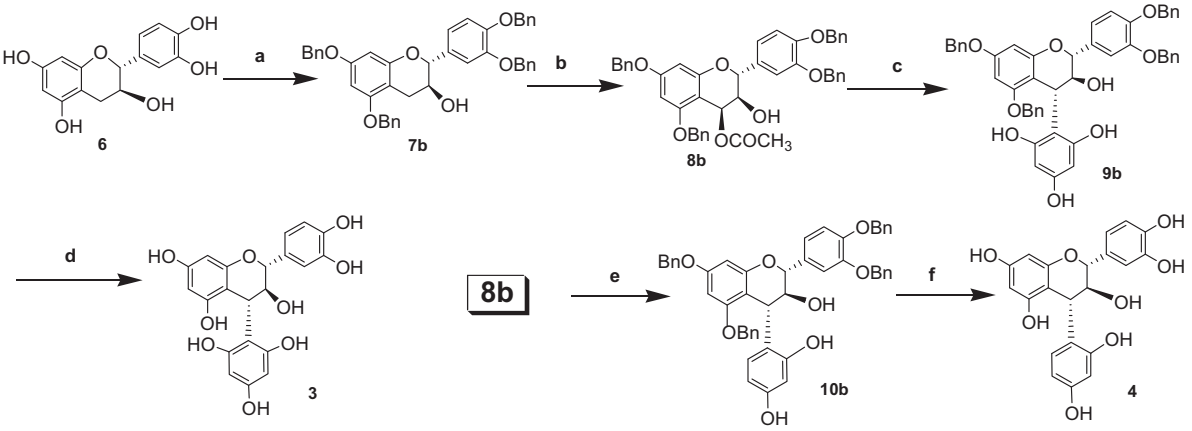

Scheme 1B. Synthesis of polyphenols (**3**–**4**) from catechin. Reagents and conditions: (a) BnBr, K_2CO_3, DMA, rt, 24 h; (b) $Pb(OAc)_4$, benzene/acetic acid (1:1), rt, 18 h; (c) phloroglucinol, LiBr, THF/DCM (1:1), reflux, 70 °C, 24 h; (d) 20% $Pd(OH)_2$–C, THF/MeOH/H_2O (20:1:1), H_2 (2 bar), 4 h; (e) resorcinol, LiBr, THF/DCM (1:1), reflux, 70 °C, 24 h; (f) 30% Pd–C, dry ethanol, H_2 (2 bar), 4 h.

Table 1
Comparison of coupling constants

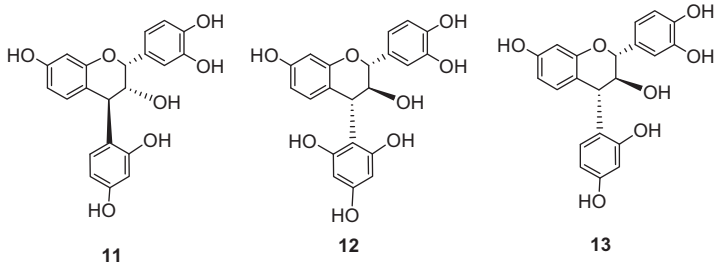

Coupling constants in Hz	9a	10a	11	9b	10b	12	13
J_{3-4}	3.6	3.6	3.8	9.6	9.2	9.8	10.0
J_{2-3}	s	s	<1	8.8	7.6	10.0	9.0

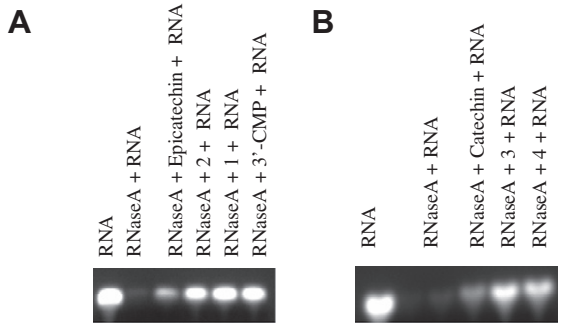

Figure 2. RNase A inhibition study for (A) epicatechin derivatives and (B) catechin derivatives.

by the enzyme after 30 min are found to be much higher compared to that of the enzyme preincubated with the compounds. Maintaining the same inhibitor concentration for all the compounds, the percent inhibition values in the histogram (Fig. 3) indicates that phloroglucinol epicatechin/catechin conjugates exhibit greater potency in inhibition of ribonucleolytic activity of RNase A compared to resorcinol epicatechin/catechin conjugates. 3′-CMP, a standard inhibitor of RNase A shows 35% inhibition of ribonucleolytic activity of RNase A where as the percent inhibition values are very low for epicatechin and catechin (~10%) as shown in Figure 3. The trend clearly reflects the contribution of phenolic OH groups in the inhibition of ribonuclease A.

2.3. Kinetic study

To ascertain the type of inhibition and inhibition constants of the synthesized compounds (**1–3**), the kinetic experiments were conducted. The reaction rate/substrate concentration is plotted against reaction rate with varying inhibitor concentrations following the Eadie–Scatchard plot using 2′, 3′-cyclic cytidine monophosphate as the substrate. The modified polyphenols (**1, 2** and **3**) behave as non-competitive inhibitors of RNase A with inhibition constants of 278 ± 1.5 μM, 390 ± 3 μM and 290 ± 2.5 μM, respectively, as obtained from the Eadie–Scatchard plot (Fig. 4). The

Table 2
Inhibition potency from the relative intensity values of the residual tRNA bands

Compounds	Epicatechin	Catechin	**1** (PEC)	**2** (REC)	**3** (PC)	**4** (RC)	3′-CMP
Relative intensity with respect to the control in the first lane	0.2949	0.3307	0.7038	0.6586	0.6987	0.6115	0.7099

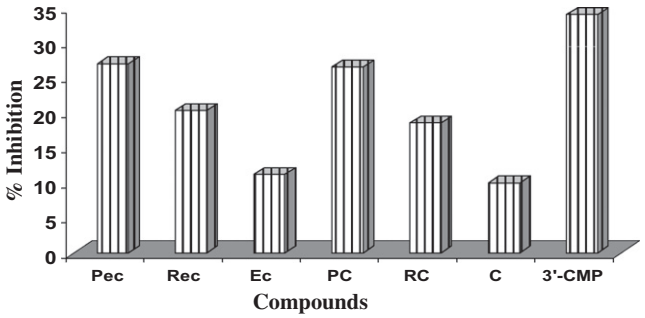

Figure 3. Ribonucleolytic inhibition of RNase A by synthesized polyphenols. RNase A and compound concentration are 5.6 μM and 0.54 mM, respectively.

reported inhibition constant value for epicatechin, a non-competitive inhibitor of RNase A is 1336 μM.[10,11] The order of inhibition constants correlates to that of agarose gel and precipitation assay. The results from the inhibition kinetics of the compounds as well as those from agarose gel and precipitation assays supports the fact that increasing number of phenolic OH groups enhances the inhibition potency of the synthesized polyphenols.

2.4. CD studies

The results from the kinetic experiments indicate a non-competitive mode of inhibition that prompted us to further probe the effects of these compounds on the secondary structure of RNase A by CD experiments. The CD spectroscopic studies indicate that polyphenol binding to RNase A results in slight perturbations in the secondary structure of the protein (Supplementary data).

2.5. Fluorescence studies

To further elucidate the binding parameters the fluorescence quenching studies (Fig. 5) of the ribonuclease A upon complexation with the polyphenols (**1**–**4**) were performed at room temperature. Here we found a gradual decrease in tyrosine fluorescence of RNase A upon excitation at 280 nm with increasing concentration of the ligand molecules. The observed quenching indicates a close proximity of the polyphenols to the environment of the protein fluorophore. The quenching data was fitted to the Stern–Volmer equation and the quenching constants (K_{SV}) (Table 3) were obtained from the Stern–Volmer plot. The bimolecular quenching constants (k_q) for all the synthesized polyphenols have been calculated using the equation $K_{sv} = k_q\ \tau_0$. The values are found to be 100–300 times higher than the limiting value of $1 \times 10^{10}\ M^{-1}\ s^{-1}$. This implies that the observed quenching is due to a static process with complex formation involving specific binding. Moreover, the linearity of the Stern–Volmer plot supports the same. The binding constants (K_b) and the number of binding sites (n) have been obtained from the Scatchard plot for all the synthesized polyphenols upon binding to the RNase A. All the compounds have the binding constant values in the order of $10^4\ M^{-1}$. Moreover, the binding constant values for the compounds **1** and **3** (containing phloroglucinol moiety) are slightly higher compared to compounds **2** and **4** (resorcinol derivatives).

2.6. Docking analysis

The protein–ligand docking studies were then performed to gain some insight into the amino acids involved in the interactions with the polyphenols. The mode of binding observed in the docking experiments for the polyphenols with RNase A corroborates our experimental findings. The docked conformations of the RNase A polyphenol complexes shown in Figure 6 reveal that the polyphenols do not dock to the ribonucleolytic site of RNase A (1FS3) which is in agreement with our experimental observations. Moreover, we find that all the synthesized compounds (**1**–**4**) are in close proximity to Tyr 92 of the RNase A. The possible hydrogen bonding distances have been calculated for all the compounds (Supplementary data).

To further probe the nature of the ligand binding pockets we calculated the change in ASA of the interacting residues in the complexed and uncomplexed forms. As expected there is no change in the ASA of the catalytic residues, His 12, Lys 41 and His 119 that form part of the P_1 binding site. Interestingly the change in ASA of Tyr 92 is quite high for all the RNase A polyphenol complexes. The results of these calculations are given in Table 4.

Calculations for the expected values of the association constants from docking studies have been obtained using PEARLS. The order of K_a values calculated using PEARLS (Fig. 7A) follows the same order as obtained from our experimental studies (Fig. 7B). High K_a values for modified polyphenols from PEARLS corroborate our experimental data, that is, high percent inhibition values. Thus we can find a direct correlation between the experimental and theoretical data.

2.7. Antiangiogenic activity

It has been reported that RNase inhibitors are also likely inhibitors of the angiogenic activity of angiogenin since the enzymatic activity is essential for the biological activity.[15] To check the effectiveness of the epicatechin based polyphenols **1** and **2**, they were screened by the chorioallantoic membrane (CAM) assay for inhibition of angiogenin-induced angiogenesis. The effect on the growth of blood vessels by the synthesized polyphenols **1** and **2** and on angiogenin-induced angiogenesis has been checked. In Figure 8 the blood vessel growth in presence of angiogenin

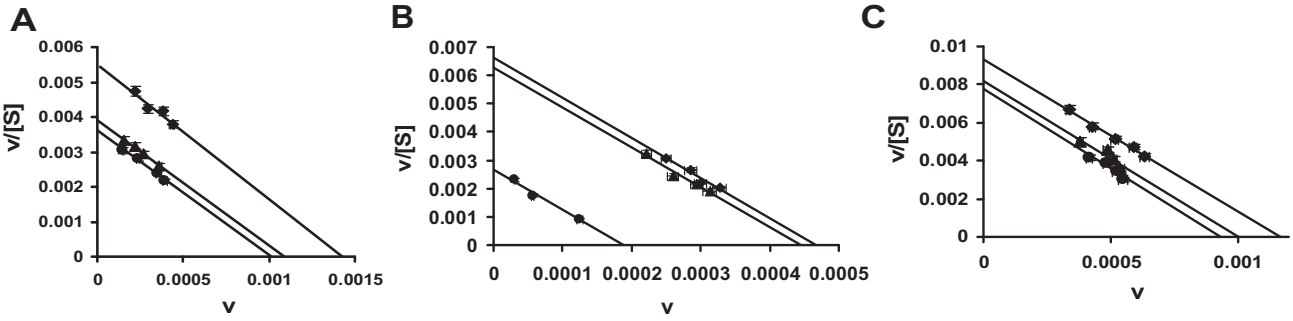

Figure 4. Eadie–Scatchard plot for inhibition of RNaseA by (A) 1: concentrations are 0 μM (■), 4 μM (▲), 12 μM (●), (B) 2: concentrations are 0 μM (■), 10 μM (▲), 50 μM (●) and (C) 3: concentrations are 0 μM (■), 4 μM (▲), 10 μM (●).

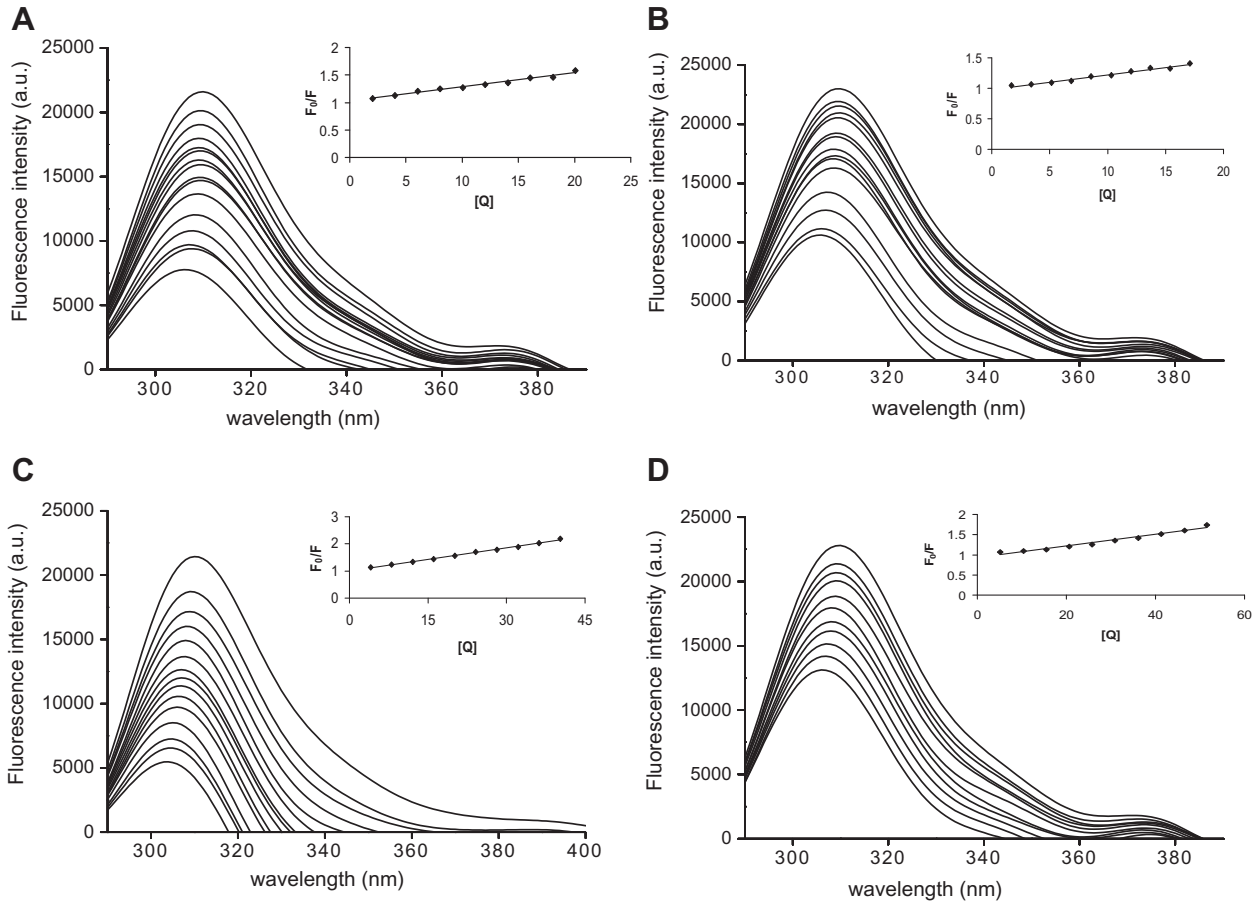

Figure 5. The fluorescence emission spectra of RNase A in absence (top) and presence of (A) the compound **1** (2–20 μM), (B) the compound **2** (1.71–17.1 μM), (C) the compound **3** (4.025–40.25 μM) and (D) the compound **4** (5.16–51.6 μM). Inset: Stern–Volmer plot of RNase A upon binding to (A) compound **1**, (B) compound **2**, (C) compound **3** and (D) compound **4**.

Table 3
The quenching and the binding constants of **1**–**4** with RNase A

Compounds	K_{sv} (10^4 M^{-1})	K_b (10^4 M^{-1})	n (number of binding sites)
1	3.64	6.76	0.66
2	2.39	2.42	1.1
3	2.83	3.14	0.63
4	1.44	1.37	0.81

preincubated with compounds **1** (150 μM) and **2** (150 μM) is suppressed compared to angiogenin (5 μM) (Fig. 8B) itself. The density of the blood vessel formation has been analyzed by Axiovision Rel. 4.6 software and a comparative histogram is given in Figure 9. The results indicate that the compounds that are inhibitors of the ribonuclease A do lead to an inhibition of angiogenic activity of the angiogenin.

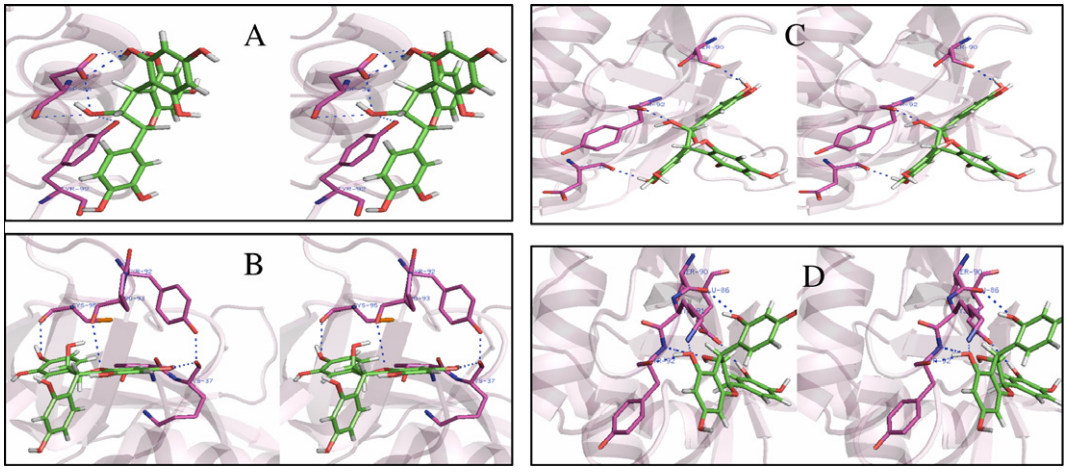

Figure 6. Stereo view of docked conformations of the polyphenols with Ribonuclease A (1FS3). Possible hydrogen bonds are shown as dashed lines. Panels correspond to (A) **1**, (B) **2**, (C) **3** and (D) **4**.

Table 4
Change in Accessible Surface Area (ΔASA) in Å^2 of the interacting residues of RNase A (uncomplexed), and its complexes with the compounds **1**–**4**

Amino acid residue	Compound number			
	1	**2**	**3**	**4**
Lys 37				
Asp 38	61.21		12.13	
Glu 86				19.82
Ser 90			17.33	14.34
Lys 91				48.04
Tyr 92	49.17	35.05	51.32	41.06
Pro 93		42.16		
Cys 95		21.94		

3. Conclusion

In conclusion, the synthesized polyphenols are found to inhibit the target enzyme, RNase A. Moreover, CAM assay results suggest that the compounds also prevent the angiogenin-induced angiogenesis. The results presented in the paper substantiate the importance of the number of phenolic hydroxyl groups in enhancing the inhibition process as compared to the parent compounds catechin and epicatechin. A clearer understanding of the mechanism or mode of binding is underway to assess how these compounds may be better modified to develop promising inhibitors of ribonuclease superfamily.

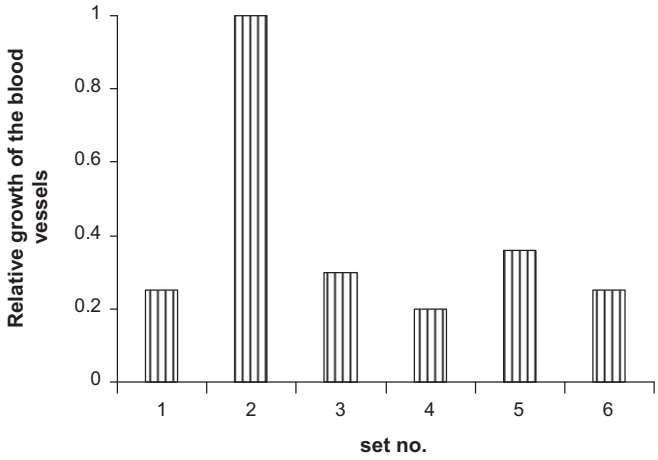

Figure 9. Relative growth of the blood vessels in presence of the synthesized polyphenols **1** and **2**. Set 1: control, 2: angiogenin, 3: angiogenin + polyphenol **1**, 4: polyphenol **1**, 5: angiogenin + polyphenol **2** and 6: polyphenol **2**.

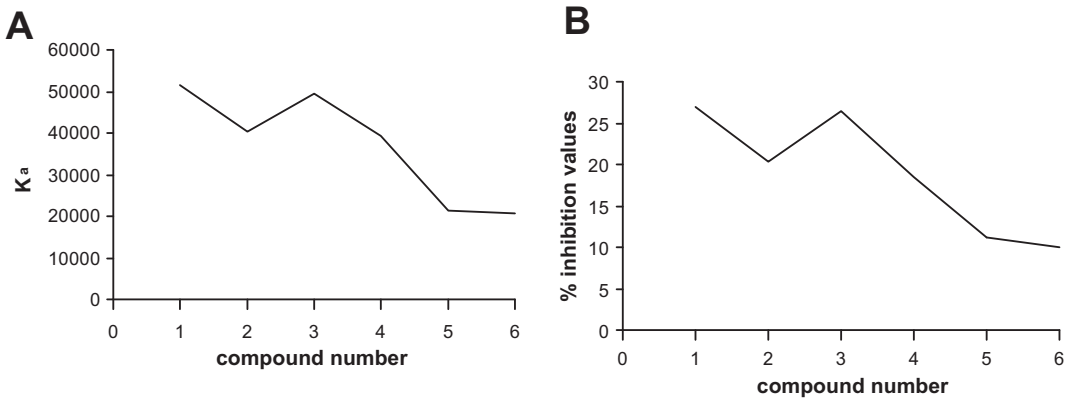

Figure 7. Comparison of experimental (A) and theoretical data (B) compounds **5** and **6** represent epicatechin and catechin.

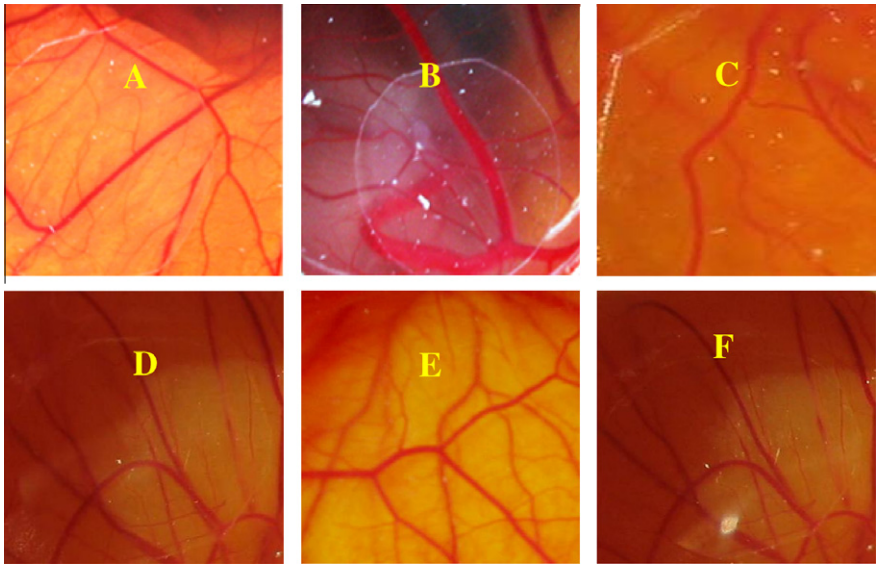

Figure 8. Effect of the polyphenols on angiogenin-induced angiogenesis: (A) control, (B) angiogenin, (C) angiogenin + **1**, (D) **1**, (E) angiogenin + **2** and (F) **2**.

4. Experimental

Ribonuclease A (RNase A), yeast tRNA, 3′-CMP, 2′, 3′-cCMP, (+)-catechin and (−)-epicatechin (EC) are from Sigma–Aldrich. All other chemicals are from SRL India. UV measurements were made using a Perkin–Elmer UV–vis spectrophotometer (Model Lambda 25). Concentrations of RNase A and 2′, 3′-cCMP (2′, 3′-cyclic cytidine monophosphate) were determined spectrophotometrically using the following data: for RNase A $\varepsilon_{278.5} = 9800\ M^{-1}\ cm^{-1}$ and for 2′, 3′-cCMP $\varepsilon_{268} = 8500\ M^{-1}\ cm^{-1}$.

4.1. Synthesis of the polyphenols (1–4)

The polyphenols (**1**, **2**) were synthesized starting with (−)-epicatechin. For compound **3** and **4** (+)-catechin was used as starting material. The benzyl ether was chosen as the protecting group because its deprotection can be done under neutral condition. Acid or base sensitive protecting groups have been avoided because of possible racemization at C-2. Based upon the literature procedure of LiBr-mediated coupling of 4-acetoxy tetrabenzyl catechin or epicatechin, the partially protected compounds were prepared which were deprotected with H_2 in presence of Pearlman's catalyst[12] or 30% Pd–charcoal to afford the target compounds.

Compound **1**: The solution of **9a** (0.04 g, 0.051 mmol) in a mixture of THF/MeOH/H_2O (20:1:1) (22 ml) were hydrogenated at 2 bar pressure over 20% $Pd(OH)_2/C$ (5 mg) for 4 h at room temperature. The reaction mixture was filtered and concentrated in vacuum to afford a pale brown solid which was further purified by precipitation in methanol ether system (0.016 g, 86%), mp 225–230 °C; δ_H[16] (MeOH-d_4): 6.91 (1H, s, Ar-H), 6.72 (2H, s, Ar-H), 6.04 (1H, s, Ar-H), 5.96 (1H, s, Ar-H), 5.83 (2H, s, Ar-H), 5.00 (1H, s, H-4), 4.48 (1H, s, H-2), 3.99 (1H, s, H-3), 3.31 (br s, OH); δ_C (MeOH-d_4): 157.0, 156.5, 155.9, 155.8, 144.8, 144.6, 130.9, 128.3, 127.1, 119.5, 114.6, 114.4, 113.6, 106.2, 105.3, 95.9, 94.8, 94.0, 82.8, 71.9, 37.0; mass: (ESI+) *m*/*z* 415.1119 (MH^+), 437.1005 (MNa^+) HRMS: calcd for $C_{21}H_{18}O_9 + H^+$ 415.1029 found 415.1033.

Compound **2**: The compound **10a** (0.04 g, 0.052 mmol) in ethanol solution (20 ml) was hydrogenated at 2 bar pressure over 30% Pd–C (5 mg) for 4 h at room temperature. The reaction mixture was filtered and concentrated in vacuum to afford a pale brown solid which was further purified by precipitation in methanol ether system (0.014 g, 79.6%), mp 205–210 °C; δ_H (MeOH-d_4): 6.85 (1H, s, Ar-H), 6.70 (1H, d, J = 8.4 Hz, Ar-H), 6.62 (1H, d, *J* = 8.4 Hz, Ar-H), 6.50 (1H, d, *J* = 8.0 Hz, Ar-H), 6.32 (1H, s, Ar-H), 6.18 (1H, dd, *J* = 8.4 Hz, Ar-H), 6.04 (1H, s, Ar-H), 5.96 (1H, s, Ar-H), 4.44 (1H, s, H-4), 4.08 (2H, s, H-2, H-3), 3.3 (br s, OH); δ_C (MeOH-d_4): 156.5, 156.4, 156.1, 155.1, 144.3, 144.0, 130.92, 130.0, 120.8, 118.0, 114.6, 113.8, 106.5, 105.9, 102.1, 100.4, 95.6, 94.3, 73.8, 70.0, 38.3; mass: (ESI+) *m*/*z* 399.1168 (MH^+), 421.1000 (MNa^+) HRMS: calcd for $C_{21}H_{18}O_8 + H^+$ 399.1080 found 399.1085.

Compound **3**: The solution of **9b** (0.04 g, 0.051 mmol) in a mixture of THF/MeOH/H2O (20:1:1) (22 ml) was hydrogenated at 2 bar pressure over 20% $Pd(OH)_2/C$ (5 mg) for 4 h at room temperature. The reaction mixture was filtered and concentrated in vacuum to afford a pale brown solid which was further purified by precipitation in methanol ether system. (0.015 g, 80%), mp 209–214 °C; δ_H (MeOH-d_4): 6.94 (1H, s, Ar-H), 6.84–6.74 (2H, m, Ar-H), 5.98–5.83 (4H, m, Ar-H), 4.6 (1H, br s, H-4), 4.44 (2H, br s, H-2, H-3), 3.30 (br s, OH); δ_C (MeOH-d_4): 157.2, 155.9, 155.8, 155.4, 144.7, 144.0, 131.2, 128.3, 127.1, 119.3, 114.6, 114.4, 113.3, 106.2, 105.3, 95.8, 94.8, 94.0, 82.6, 71.6, 37.5; mass: (ESI+) *m*/*z* 415 (MH^+), 437 (MNa^+), HRMS: calcd for $C_{21}H_{18}O_9 + H^+$ 415.1029 found 415.1037.

Compound **4**: The compound **10b** (0.03 g, 0.039 mmol) in ethanol solution (20 ml) was hydrogenated at 2 bar pressure over 30% Pd–C (5 mg) for 4 h at room temperature. The reaction mixture was filtered and concentrated in vacuum to afford a pale brown solid which was further purified by precipitation in methanol ether system to obtain compound **4** (0.013 g, 74.5%), 203–208 °C; δ_H (MeOH-d_4): 6.67 (1H, s, Ar-H), 6.58 (2H, s, Ar-H), 6.44 (1H, t, *J* = 4.0 Hz, Ar-H), 6.13 (1H, s, Ar-H), 6.03 (1H, dd, *J* = 2.0, 2.4 Hz, Ar-H), 5.81 (1H, s, Ar-H), 5.75 (1H, d, *J* = 2.0 Hz, Ar-H), 4.29 (1H, d, J = 9.2, H-4), 4.12 (1H, d, *J* = 8.4 Hz, H-2), 3.75 (1H, ABq, *J* = 8.4, H-3), 3.12 (br s, OH). δ_C (MeOH-d_4): 157.7, 156.6, 156.1, 155.2, 144.9, 144.5, 129.6, 127.8, 121.0, 119.6, 114.9, 114.4, 107.6, 107.5, 103.8, 103.0, 96.9, 95.5, 81.8, 76.9, 40.2; mass: (ESI+) *m*/*z* 399 (MH^+), 421 (MNa^+), HRMS: calcd for $C_{21}H_{18}O_8 + H^+$ 399.1080 found 399.1084.

Compound **9a**: To a solution of 4-acetoxy tetrabenzyl epicatechin (**8a**) (0.075 g, 0.1 mmol) in a mixture of CH_2Cl_2 and THF (2 ml each) phloroglucinol (0.063 g, 0.5 mmol) was added followed by LiBr (0.043 g, 0.5 mmol). The mixture was refluxed for 24 h and partitioned between ethyl acetate and water. The organic layer was evaporated to dryness. The crude residue thus obtained was purified by flash column chromatography using 5% methanol in dichloromethane as eluent to afford compound **9a** (0.06 g, 79.1%); δ_H ($CDCl_3$): 7.38–6.91 (25H, m, Ar-H), 6.37 (1H, s, Ar-H), 6.28 (1H, s, Ar-H), 5.12–5.02 (8H, m, 4 × OCH_2Ph), 4.92 (1H, d, *J* = 3.6 Hz, H-4), 4.62 (1H, s, H-2), 4.06 (1H, s, H-3), 1.26 (br s, OH); mass: (ESI+) *m*/*z* 775 (MH^+); HRMS: calcd for $C_{49}H_{42}O_9 + H^+$ 775.2907 found 775.2912.

Compound **9b**: To a solution of 4-acetoxy tetrabenzyl catechin (**8b**) (0.080 g, 0.11 mmol) in a mixture of CH_2Cl_2 and THF (2 ml each) phloroglucinol (0.071 g, 0.55 mmol) was added followed by LiBr (0.047 g, 0.55 mmol). The mixture was refluxed for 24 h and partitioned between ethyl acetate and water. The organic layer was evaporated to dryness. The crude residue thus obtained was purified by flash column chromatography using 5% methanol in dichloromethane as eluent to afford compound **9b** (0.060 g, 76.2%). δ_H ($CDCl_3$): 7.44–7.22 (20H, m, Ar-H), 7.05 (1H, s, Ar-H), 6.96–6.89 (4H, m, Ar-H), 6.27 (2H, s, Ar-H), 5.19–4.77 (8H, m, 4 × OCH_2Ph), 4.55 (1H, d, *J* = 9.6 Hz, H-4), 4.47 (1H, d, *J* = 8.8 Hz, H-2), 4.01 (1H, m, H-3), 3.30 (br s, OH) ; mass: (ESI^+) *m*/*z* 775 (MH^+); HRMS: calcd for $C_{49}H_{42}O_9 + H^+$ 775.2907 found 775.2914.

Compound **10a**: To a solution of **8a** (0.071 g, 0.098 mmol) in a mixture of CH_2Cl_2 and THF (2 ml each) resorcinol (0.054 g, 0.49 mmol) was added followed by LiBr (0.042 g, 0.49 mmol). The mixture was refluxed for 24 h and partitioned between ethyl acetate and water. The organic layer was evaporated to dryness. The crude oily residue thus obtained was purified by flash column chromatography using 5% methanol in dichloromethane as eluent to afford compound **10a** (0.047 g, 62%). δ_H ($CDCl_3$): 7.45–6.80 (24H, m, Ar-H), 6.62 (1H, d, *J* = 7.6 Hz, Ar-H), 6.36–6.20 (3H, s, Ar-H), 5.17–4.83 (8H, m, 4 × OCH_2Ph), 4.80 (1H, d, *J* = 3.6 Hz, H-4), 4.60 (1H, s, H-2), 4.06 (1H, s, H-3), 2.14 (br s, OH); mass: (ESI^+) *m*/*z* 759 (MH^+); HRMS: calcd for $C_{49}H_{42}O_8 + H^+$ 759.2958 found 759.2964.

Compound **10b**: To a solution of **8b** (0.071 g, 0.098 mmol) in a mixture of CH_2Cl_2 and THF (2 ml each) resorcinol (0.054 g, 0.49 mmol) was added followed by LiBr (0.042 g, 0.49 mmol). The mixture was refluxed for 24 h and partitioned between ethyl acetate and water. The organic layer was evaporated to dryness. The crude residue thus obtained was purified by flash column chromatography using 5% methanol in dichloromethane as eluent to afford compound **10b** (0.047 g, 62%). δ_H ($CDCl_3$): 7.40–6.73 (25H, m, Ar-H), 6.48 (1H, d, *J* = 8.4 Hz, Ar-H), 6.33 (1H, d, *J* = 2.0 Hz, Ar-H), 6.25 (1H, d, *J* = 2.0 Hz, Ar-H), 5.12–4.96 (8H, m, 4 × OCH_2Ph), 4.54 (1H, d, *J* = 9.2 Hz, H-4), 4.38 (1H, d, *J* = 7.6 Hz, H-2), 3.9–3.83 (1H, m, H-3), 3.30 (br s, OH); mass: (ESI^+) *m*/*z* 759 (MH^+); HRMS: calcd for $C_{49}H_{42}O_8 + H^+$ 759.2958 found 759.2962.

4.2. Agarose gel based assay

Comparative inhibition of ribonucleolytic activity of ribonuclease A by the synthesized compounds **1–4** was estimated by agarose gel electrophoresis. The degradation of tRNA was monitored in this method. 20 μl of RNase A (0.8 μM) was mixed with 20 μl each of the compounds **1–4**, (+)-catechin, (−)-epicatechin (EC) and 3′-CMP having 4 mM concentration, respectively. The resulting solutions were incubated for 4 h along with the control set containing 20 μl of RNase A and 20 μl buffer. 20 μl tRNA (7.2 mg/ml tRNA freshly prepared in RNase free water) was added to each of incubated mixture after completion of 4 h. The resulting solutions were incubated for another 30 min. 10 μl of sample buffer consisting of 10% glycerol and 0.025% bromophenol blue in water were added to the mixtures and 15 μl of it was extracted and loaded onto a 1.1% agarose gel. The known inhibitor of RNase A, 3′-CMP, (+)-catechin, (−)-epicatechin (EC) were used for comparison. The undegraded tRNA was visualized by ethidium bromide staining under UV light.

4.3. Precipitation assay

Inhibition of the ribonucleolytic activity of RNase A was assayed by the precipitation assay as described by Bond.[14] In this method 10 μl of RNase A (5.6 μM) was mixed with 10 μl of 0.54 mM each of epicatechin, catechin, the polyphenols (**1–4**) and 3′-CMP to a final volume of 100 μl and incubated for 2 h at 37 °C. 20 μl of the resulting solutions from the incubated mixtures were then mixed with 40 μl of tRNA (5 mg/ml tRNA freshly dissolved in RNase A free water), 40 μl of Tris buffer of pH 7.5 containing 5 mM EDTA and 0.5 mg/ml HSA. After incubation of the reaction mixture at 25 °C for 30 min, 200 μl of ice-cold 1.14 N perchloric acid containing 6 mM uranyl acetate was added to quench the reaction. The solution was then kept in ice for another 30 min and centrifuged at 4 °C at 12,000 rpm for 5 min. 100 μl of the supernatant was taken and diluted to 1 ml. The change in absorbance at 260 nm was measured and compared with a control set.

4.4. Kinetic study

The inhibition of RNase A by the polyphenols was assessed individually by a spectrophotometric method as described by Anderson et al.[17] The assay was performed in oligo vinylsulphonic acid free (using the method as described by Smith et al.[18]) 0.1 M Mes–NaOH buffer, pH 6.0 containing 0.1 M NaCl using 2′, 3′-cCMP as the substrate. For the compounds **1**, 2 and **3** the substrate concentrations ranged from 0.0463 to 0.139 mM, 0.0544 to 0.1632 mM and 0.05 to 0.1505 mM, respectively, and the inhibitor concentration ranges for compounds **1** and 3 were from 0 to 0.012 mM and 0 to 0.05 mM for compound **2**. The RNase A concentration used was 12 μM. A rearranged form of the Michaelis–Menten equation leading to the Eadie–Scatchard plot has been used to confirm the K_m, K_i and V_{max} values. The reaction rate/substrate concentration was plotted against reaction rate (Eadie–Scatchard plot)[19] at a constant inhibitor concentration according to the equation:

$$v/[S] \approx -v/K_s + V_{max}/K_s$$

where v is the initial velocity, $[S]$ the substrate concentration, K_s the Michaelis constant and V_{max} the maximum velocity.

4.5. Fluorescence quenching studies

All steady state fluorescence measurements were carried out using Spex Fluoromax-3 Spectrofluorimeter. The bandwidth of both excitation and emission slits were 2 nm with an integration time of 0.3 s. Fluorescence quenching titrations were performed in a 1 cm quartz cuvette by successive addition of compounds **1–4** to a solution of the RNase A (7.04 μM) in phosphate buffer, pH 7, respectively. The control spectra were recorded for all the compounds and the spectra were corrected accordingly. To minimize the inner filter effect a low concentration of RNase A was used and checked by using $F_{corr} = F_{obs} \times \text{antilog}\ [(OD_{ex} + OD_{em})/2]$[20] where F_{corr} and F_{obs} are the corrected and observed fluorescence intensities. The Stern–Volmer plot[20] was used to ascertain the quenching constant values following the equation given below.

$$F_o/F \approx 1 + K_{sv}[Q]$$

where F_0 and F stand for the relative fluorescence intensities in the absence and presence of quencher, $[Q]$ is the quencher concentration and K_{SV} is the Stern–Volmer quenching constant. Later the binding constants and the number of binding sites of all the synthesized polyphenols (**1–4**) upon binding to RNase A were evaluated following the Scatchard plot[21–23] using the equation.

$$v/L_f \approx nK - vK$$

where v is the moles of ligand bound per mole of protein, L_f is the molar concentration of free ligand, n the binding site multiplicity per class of binding sites and K the binding constant.

4.6. Docking studies

The crystal structure of RNase A (PDB entry 1FS3)[24] was downloaded from the Protein Data Bank.[25] We have chosen 1FS3 for the docking studies since this is the structure of the wild type bovine pancreatic RNase A and should be able to appropriately complement our experimental results that have been conducted with the same protein. The 3D structures of the compounds were generated by Sybyl6.92 (Tripos, St. Louis) and their energy minimized conformations were obtained with the help of the TRIPOS force field using Gasteiger–Hűckel charges with a gradient of 0.005 kcal/mole. The FlexX software as part of the Sybyl suite was used for docking of the compounds to RNase A. The ranking of the generated solutions is performed using a scoring function that estimates the free binding energy ΔG of the protein–ligand complex.[26] PyMol[27] was used for visualization of the docked conformations. The theoretical value of the association constants (K_a) of the docked structures of the protein–ligand complexes was computed using PEARLS,[28] which computes interaction energies for receptor–ligand systems.

4.7. Accessible surface area calculations

The accessible surface area (ASA) of RNase A (uncomplexed) and their docked complexes with the compounds **1–4** were calculated using the program NACCESS.[29] The structures corresponding to the minimum score as obtained from the FlexX analysis of the protein–ligand docked structures were chosen in each case. Composite coordinates of the polyphenols and RNase A were generated to form the docked complex. The change in ASA for residue, i was calculated using: $\Delta ASA^i = ASA^i_{RNase\ A} - ASA^i_{RNase\ A-polyphenol}$. If a residue lost more than 10 Å^2 ASA when going from the uncomplexed to the complexed state it was considered as being involved in the interaction.

4.8. CAM assay

The effect of the compounds on angiogenin-induced angiogenesis was assessed by the chick embryo chorioallantoic membrane (CAM) assay following the method described by Fett et al.[3] The chorioallantoic membrane of the chicken egg was exposed carefully by drilling a small hole through the shell on day 2. 10 μl aliquots of angiogenin and angiogenin mixed with compounds were

placed on transparent disc and dried under laminar flow. The discs were then inverted over the chorioallantoic membrane on day 10 and the response was assayed after 48 h. The density of blood vessel formation was compared with a control set.

Acknowledgements

A.B. thanks DST for a research Grant. S.D.G. is grateful to Council for Scientific and Industrial Research (CSIR) (01(2115)/07/EMR-II), for funding. S.D. is thankful to IIT, Kharagpur for a fellowship. Central Research Facility, IIT Kharagpur is acknowledged for providing experimental facilities.

Supplementary data

Supplementary data associated with this article can be found, in the online version, at doi:10.1016/j.bmc.2010.06.077.

References and notes

1. Richards, F. M.; Wyckoff, H. W. *The Enzymes*, 3rd ed.; Academic press: New York, 1971. pp 647–806.
2. Raines, R. T. *Chem. Rev.* **1998**, *98*, 1045.
3. Fett, J. W.; Strydom, D. J.; Lobb, R. R.; Alderman, E. M.; Bethune, J. L.; Riordan, J. F.; Vallee, B. L. *Biochemistry* **1985**, *20*, 5480.
4. Sorrentino, S.; Glitz, D. G.; Hamann, K. J.; Loegering, D. A.; Checkel, J. L.; Gleich, G. J. *J. Biol. Chem.* **1992**, *267*, 14859.
5. Matousek, J. *Comp. Biochem. Physiol. C.* **2001**, *129*, 175.
6. Loverix, S.; Steyaert, J. *Curr. Med. Chem.* **2003**, *10*, 779.
7. Dreostic, I. E.; Wargovich, M. J.; Yang, C. S. *Crit. Rev. Food Sci.* **1997**, *37*, 761.
8. Cai, Y.; Ma, L.; Hou, L.; Zhou, B.; Yang, L.; Liu, Z. *Chem. Phys. Lipids* **2002**, *120*, 109.
9. Balentine, D. *Food Sci.* **1997**, *37*, 691.
10. Ghosh, K. S.; Maiti, T. K.; Dasgupta, S. *Biochem. Biophys. Res. Commun.* **2004**, *325*, 807.
11. Ghosh, K. S.; Maiti, T. K.; Debnath, J.; Dasgupta, S. *Proteins* **2007**, *69*, 566.
12. Kozikowski, A. P.; Tuckmantel, W.; Bottcher, G.; Romanczyk, L. J., Jr. *J. Org. Chem.* **2003**, *68*, 1641; Saito, A.; Doi, Y.; Tanaka, A.; Matsuura, N.; Ubukata, M.; Nakajima, N. *Bioorg. Med. Chem.* **2004**, *12*, 4783.
13. (a) Botha, J. J.; Ferreira, D.; Roux, D. G. *J. Chem. Soc., Chem. Commun.* **1978**, 698; (b) Romanczyk, L. J.; Basak, A.; Townsend, C. A. PCT Int. Appl., 2000, 81, pp CODEN: PIXXD2 WO 0063201 A1 20001026.; (c) Kawamoto, H.; Nakatsubo, F.; Murakami, K. *Synth. Commun.* **1996**, *26*, 531; (d) Basak, A.; Mandal, S.; Bandhyopadhyay, S. *Bioorg. Med. Chem. Lett.* **2003**, *13*, 1083.
14. Bond, M. D. *Anal. Biochem.* **1988**, *173*, 166.
15. Maiti, T. K.; De, S.; Dasgupta, S.; Pathak, T. *Bioorg. Med. Chem.* **2006**, *14*, 1221.
16. All ^{1}H and ^{13}C NMR spectra were recorded at 400 and 100 MHz, respectively.
17. Anderson, D. G.; Hammes, G. G.; Walz, F. G. *Biochemistry* **1968**, *7*, 1637.
18. Smith, B. D.; Soellner, M. B.; Raines, R. T. *J. Biol. Chem.* **2003**, *278*, 20934.
19. Segel, I. H. *Enzyme Kinetics*; John Wiley & Sons, 1993.
20. Lakowicz, J. R. *Principles of Fluorescence Spectroscopy*; Springer: New York, 2006.
21. Scatchard, G. *Ann. N.Y. Acad. Sci.* **1949**, *51*, 660.
22. Klotz, I. M.; Hunstone, D. L. *Biochemistry* **1971**, *10*, 3065.
23. Kraak, J. C.; Busch, S. *J. Chromatogr.* **1992**, *608*, 257.
24. Chatani, E.; Hayashi, R.; Moriyama, H.; Ueki, T. *Protein Sci.* **2002**, *11*, 72.
25. Berman, H. M.; Westbrook, J.; Feng, Z.; Gilliland, G.; Bhat, T. N.; Weissig, H.; Shindyalov, I. N.; Bourne, P. E. *Nucleic Acids Res.* **2000**, *28*, 235.
26. Rarey, M.; Kramer, B.; Lengauer, T.; Klebe, G. *J. Mol. Biol.* **1996**, *261*, 470.
27. DeLano, W. L. The PyMOL Molecular Graphics System. DeLano Scientific: San Carlos, CA, 2004, <http://pymol.sourceforge.net/>.
28. Han, L. Y.; Lin, H. H.; Li, Z. R.; Zheng, C. J.; Cao, Z. W.; Xie, B.; Chen, Y. Z. *J. Chem. Inf. Model.* **2006**, *46*, 445.
29. Hubbard, S. J.; Thornton, J. M. *'NACCESS' Computer Program*; Department of Biochemistry and Molecular Biology, University College: London, 1993.